Bioinspired Fog Capture and Channel Mechanism Based on the Arid Climate Plant *Salsola crassa*

M. Gürsoy[a], M. T. Harris[b], J. O. Downing[b], S. N. Barrientos-Palomo[b], A. Carletto[b], A. E. Yaprak[c], M. Karaman[a†], and J. P. S. Badyal[b†*]

[a] Chemical Engineering Department, Selçuk University, Konya 42075, Turkey

[b] Chemistry Department, Science Laboratories, Durham University, Durham DH1 3LE, England, UK

[c] Department of Biology, Faculty of Science, Ankara University, Ankara 06100, Turkey

† These authors have made equal contributions.

* Corresponding author email: j.p.badyal@durham.ac.uk

GRAPHICAL ABSTRACT

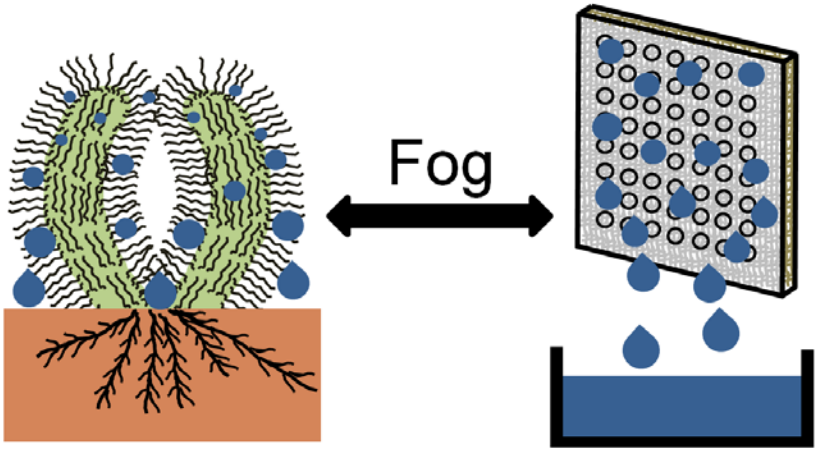

ABSTRACT

Salsola crassa plant hairs collect fog in their natural arid climate habitat through the capture and growth of water droplets. These then, either drip onto the ground below due to gravity, or coalesce into larger attached water droplets, whilst concurrently rolling downwards along the curvature of the *Salsola crassa* leaf (fog collection and water channelling mechanism). Non-woven and cotton fibrous materials are shown to mimic the fog harvesting behaviour of *Salsola crassa* hairs, where the overall mist collection efficiency can be enhanced by over 300 percent through the incorporation of multiple length scale (hierarchical) channel structures in conjunction with hydrophobic surface functionalisation.

KEYWORDS

Fog harvesting; water collection; bioinspired; hierarchical length-scales; *Salsola crassa*.

HIGHLIGHTS

- *Salsola crassa* plant collects fog through the capture and growth of water droplets.

- Fibrous materials mimic the fog harvesting behaviour of the *Salsola crassa* plant.

- Hierarchical structures and hydrophobicity enhance mist collection efficiency.

1. INTRODUCTION

Around one billion people in the world lack access to clean drinking water, with many living in arid or semi-arid regions[1]. Additionally, three out of four jobs worldwide are water-dependent, and lack of access is limiting economic growth in some developing countries[2]. Water collection from the air (moisture condensation and fog harvesting) is a potentially cheap and environmentally-sustainable approach in arid regions of the world suffering from shortages of potable water required for drinking and agricultural purposes[3,4,5,6].

Existing large-scale (50 m^2) fog collection systems are based upon vertically hanging flat screen nets (Raschel meshes, fibre and gap length scales are in the millimetre and centimetre ranges respectively); these are reliant upon aerodynamic drag and offer relatively low surface areas leading to ~20% efficiency[7,8]. Typical fog harvesting yields are reported to be 1–10 L m^{-2} Day^{-1}.[4] Furthermore, high wind speeds and pressure can cause sagging and plastic deformation of such manmade two-dimensional nets leading to tearing and ruptures[9]. Alternative sponge-like materials have been found to either display low fog collection efficiencies[10] or require additional steps for water recovery[11]. Fog collectors can also be found in nature, these include spindle-knots of spider silk[12], barbed surfaces of *Hordeum vulgare*[13], cactus[14], twisted spiral desert geophytes,[15] and fibrous hairs of the *Cotula fallax* plant[16].

In this article, a three-dimensional compact, high effective surface area, and multiple length scale (hierarchical) fog collection structure is described, which has been inspired by the *Salsola crassa* plant species found in arid climates, Scheme 1. *Salsola crassa* M.Bieb. subsp. *crassa* is an annual xero-halophytic plant which is found in south-west and central Asia, Ukraine, and Transcaucasia[17,18]. In Turkey, the plant's native habitat is in one of the most arid parts of the country, namely the Iğdır plain and near to Lake Tuz. In both of these regions, the average annual precipitation is very low (252 mm and 323 mm respectively). The younger plants have a pubescence of fine, entangled hairs (arachnoid indumentum) on their leaves, however these disappear by the time they become adult plants (glabrescent or glabrous). During spring (the fog season), the arachnoid indumentum most probably allows the younger plants growing from seeds to collect water and minimise loss via transpiration in such arid conditions.

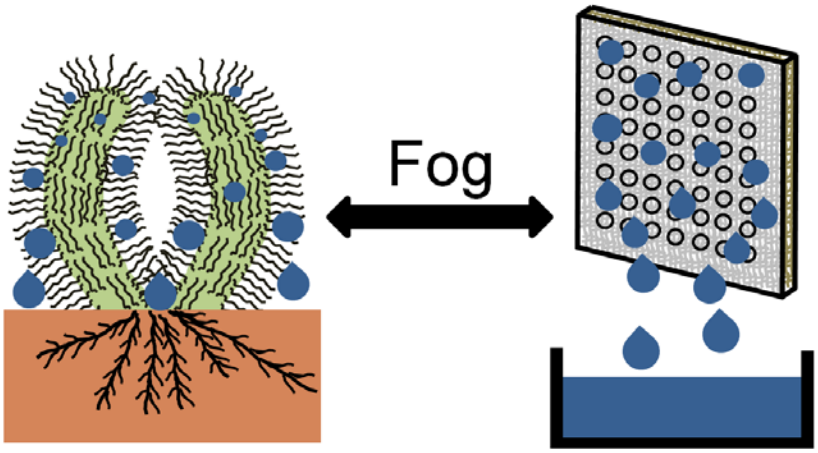

Scheme 1: Fog collection mechanism of *Salsola crassa* plant species and bioinspired fibrous water harvesting.

2. EXPERIMENTAL

2.1 Plant Species and Materials

The plant *Salsola crassa* M.Bieb. subsp. *crassa* was sourced near to Lake Bolluk, located in Cihanbeyli-Konya, Turkey. Hairs (trichomes) from the leaves were removed using adhesive tape (product code AB124, Alfabant Company, Turkey). The fibrous cloth substrates employed for mist collection were: organic cotton (Apaks, 100% Pur Coton, 100 gr, S.N.003.URT.24.03.15, İpek İdrofil Pamuk San. ve Tic. A.Ş., Turkey), coarse and fine non-woven polypropylene (SDMedical50pk, SecurityDirect.co.uk), and hierarchical-coarse non-woven polypropylene (Spunbond, 70 g m^{-2} grade, Avoca Technical Ltd, UK). Flat polyethylene sheet (HDPE natural, Gilbert Curry Industrial Plastics Co Ltd., UK) was employed as a non-porous reference standard because it has very similar surface chemical properties to polypropylene.

2.2 Surface Functionalisation

Initiated chemical vapour deposition (iCVD) surface coatings were applied in a custom-built stainless steel chamber (20 cm width, 30 cm length, and 5 cm height)[19]. The chamber was connected to a two-stage rotary pump, with a butterfly-valve (MKS) located between the chamber and the pump, used to control the chamber

pressure (monitored by a capacitance Baratron pressure transducer, MKS). This was done through a proportional–integral–derivative (PID) control unit (MKS), connected to both the pressure transducer and the butterfly-valve. Monomer 1H,1H,2H,2H-perfluorodecyl acrylate (PFDA, Sigma Aldrich, 97%) and initiator di-tertbutyl peroxide (TBPO, Sigma Aldrich, 98%) were used as received, without further purification[20]. Each substrate sample was placed inside onto the base of the chamber (maintained at 35 °C using water cooling), followed by evacuation to system base pressure. Next, precursors vaporised in stainless steel vessels were fed into the chamber via needle control valves at predetermined pressures. A tungsten (Alfa Aesar, 0.375 mm diameter, 99.95%) filament array located 20 mm above the substrate surface was resistively heated using a variable transformer to initiate the polymerization reactions. Filament temperature during deposition was monitored using a K-type thermocouple (Omega) directly attached to one of the filaments. Depositions onto a reference silicon wafer were monitored using interferometry with a 632.8 nm He-Ne laser source. The deposition conditions used were as follows: 150 mtorr chamber pressure, 280 °C filament temperature, 0.5 sccm PFDA flowrate, 0.8 sccm TBPO flowrate. Upon completion of iCVD, the precursor feed valves were closed, and the chamber vented to atmosphere.

Plasmachemical surface functionalisation was carried out in a cylindrical glass chamber (5 cm diameter, 432 cm^3 volume) enclosed within a Faraday cage. This was connected to a two-stage rotary pump via a liquid nitrogen cold trap. An inductor-capacitor (L-C) impedance matching network was used to minimise the standing wave ratio (SWR), for the power transmitted from a 13.56 MHz radio frequency (RF) generator to a copper coil (10 turns, spanning 8 cm) externally wound around the glass chamber. In the case of pulsed plasma functionalisation, a signal generator was used to trigger the RF power supply, and the pulse shape monitored with an oscilloscope. Prior to each plasma deposition, the reactor was scrubbed with detergent, rinsed in propan-2-ol (99.5%, Fischer Scientific Ltd.), and further cleaned using a 50 W air plasma at 0.2 mbar pressure for 30 min. Each substrate sample was then placed into the centre of the reactor, followed by evacuation to system base pressure. Next, precursor vapour was admitted into the chamber via a needle control valve at 0.2 mbar pressure, and the electrical discharge ignited. Upon completion of plasma deposition, the precursor vapour source was switched off, and the chamber vented to atmosphere. Precursors used

were as follows: 1H,1H,2H,2H-perfluorooctyl acrylate (+95%, Fluorochem Ltd.) for hydrophobicity using a duty cycle on-period (t_{on}) of 20 μs and a duty cycle off-period (t_{off}) of 20 ms in conjunction with 40 W power (P_{on})[21], and 1-allylimidazole, (+97%, Fisher Scientific Ltd) using a duty cycle on-period (t_{on}) of 20 μs and a duty cycle off-period (t_{off}) of 1200 μs in conjunction with 30 W power (P_{on}).[22]

2.3 Characterisation

Photographs were taken using a camera (model Fujifilm FinePix S2950, Fujifilm Holdings, Japan). Higher magnification surface topography images were obtained of samples mounted onto a carbon disk supported on an aluminum holder, and coated with a 5 nm gold layer, using a scanning electron microscope (Model EVO LS 10, Carl Zeiss Microscopy Ltd).

Sessile droplet contact angle analysis was undertaken with a video capture system (Model OCA 50, DataPhysics Instruments GmbH) using 2 μL dispensation of de-ionised water for the iCVD hydrophobic samples. In the case of the PECVD hydrophobic and hydrophilic samples, sessile droplet contact angle analysis was undertaken at 20 °C with a video contact angle goniometer (VCA 2500 XE, AST Products Ltd.) using 1.0 μL droplets of high purity water (BS 3978 grade 1).

Mist collection measurements were undertaken by mounting each sample above an 11 mm inner neck diameter, 25 cm^3 volumetric flask (ISOLAB Laborgeräte GmbH), positioned on top of a mass balance, Figure 1. 0.5–6.0 μm water droplets were generated using a 6 cm^3 chamber volume nebulizer (Freely Plus Model: V5002, Atılım Sağlık A.Ş.), with air flow rate of 10 L min^{-1}, and 3.5 bar pressure, delivering a water nebulisation rate of 0.4 cm^3 min^{-1} at a velocity of 2 ms^{-1}. These droplet sizes are comparable to meteorological fog[7,23]. The distance between sample front and nebulizer was set to 4 cm. All experiments were performed at 23 °C and repeated at least three times for each substrate sample type. Mist collection experiments were also performed with the whole *Salsola crassa* plant (leaves and hairs), i.e. the ratio of collected water relative to the mass of the whole plant. Following water collection measurements by the plant, it was dried by gently patting with tissue paper, and the leaf hairs were removed using adhesive tape (product code AB124, Alfabant Company, Turkey). The difference in mass between plant with hairs after drying and plant without hairs after drying gave the calculated mass of hairs. Water collection

by the same plant specimen following hair removal was then measured in order to determine the role of the hairs (including potential hierarchical behaviour).

(a) **(b)**

Figure 1: Nebulised water mist collection apparatus: (a) side view and (b) front view.

3. RESULTS

3.1 *Salsola crassa* Plant

During fog episodes in its native habitat, the hydrophobic hairy leaves of *Salsola crassa* were observed to collect a significant amount of water, which ran off onto surrounding soil resulting in dampness, Figure 2. The light green leaves are circular in cross-section and shaped like a finger, typically 10–40 mm long (including the fine hairs) and 5–10 mm in diameter (2.5–4.5 mm after the hairs have been removed). These leaves curl inwards, so enabling them to channel water towards the stem and then the ground below. Individual hairs on these leaves measured 2–5 mm in length, and hence their entanglement provides a fibrous mesh-like structure, Figure 2. Fog collection proceeds through the growth of beaded water droplets attached to *Salsola crassa* hairs, which then either drip onto the ground due to gravity, or coalesce into larger-attached water droplets rolling along the contour of the *Salsola crassa* leaf towards the plant base (collection and channelling of water). Fog droplets bouncing off the surface were not observed. Removal of the hairs resulted in leaf wetting, indicating that the underlying leaf surface is hydrophilic (i.e. loss of

hydrophobicity), which is accompanied by a deterioration of mist collection efficiency, Figure 3.

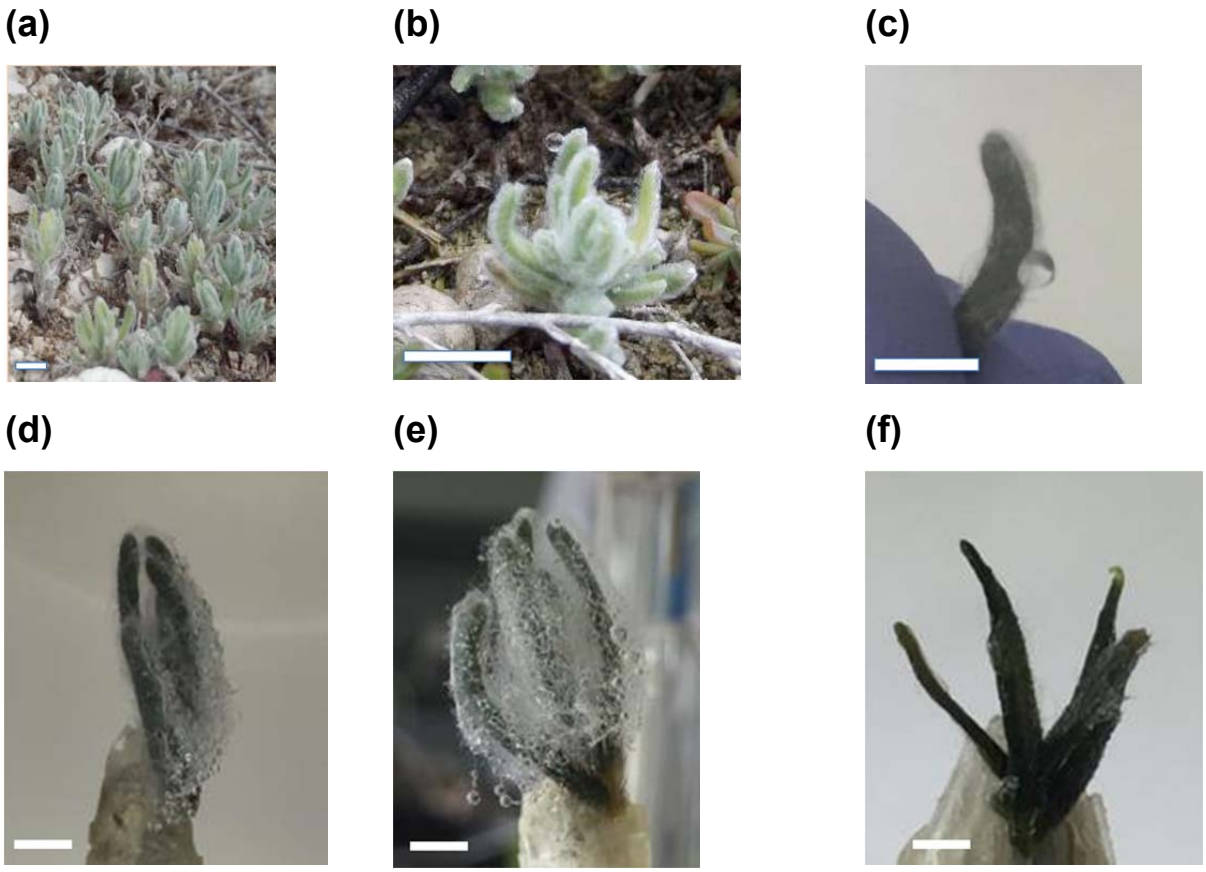

Figure 2: Photographs of *Salsola crassa*: (a)–(b) whole plants growing in natural habitat; (c) plant leaf; (d) side view, showing the front face of the plant's leaves, collecting water droplets, when directed towards the incident water mist flow from the right side of the image; (e) front view of (d); and (f) repeat of (d) using same specimen after removal of hairs. Scale bars: (a)–(b) = 30 mm; and (c)–(f) = 10 mm.

(a) **(b)**

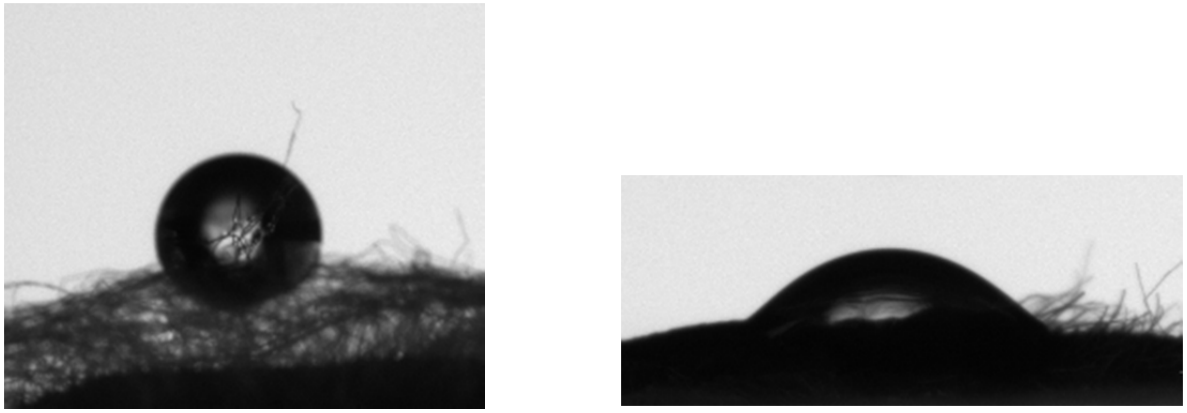

Figure 3: Water droplet contact angle images of *Salsola crassa* plant leaf: (a) 169° with hairs; and (b) 25° without hairs.

Scanning electron microscopy (SEM) showed the presence of fettuccine-like hairs on the *Salsola crassa* plant leaves, which are approximately 2–5 mm in length, 9.1 ± 1.2 μm in width, and 359 ± 125 nm in thickness, Figure 4. At higher magnification, longitudinal features running along the length of individual hairs are observed (which may enhance mist collection[16,24]).

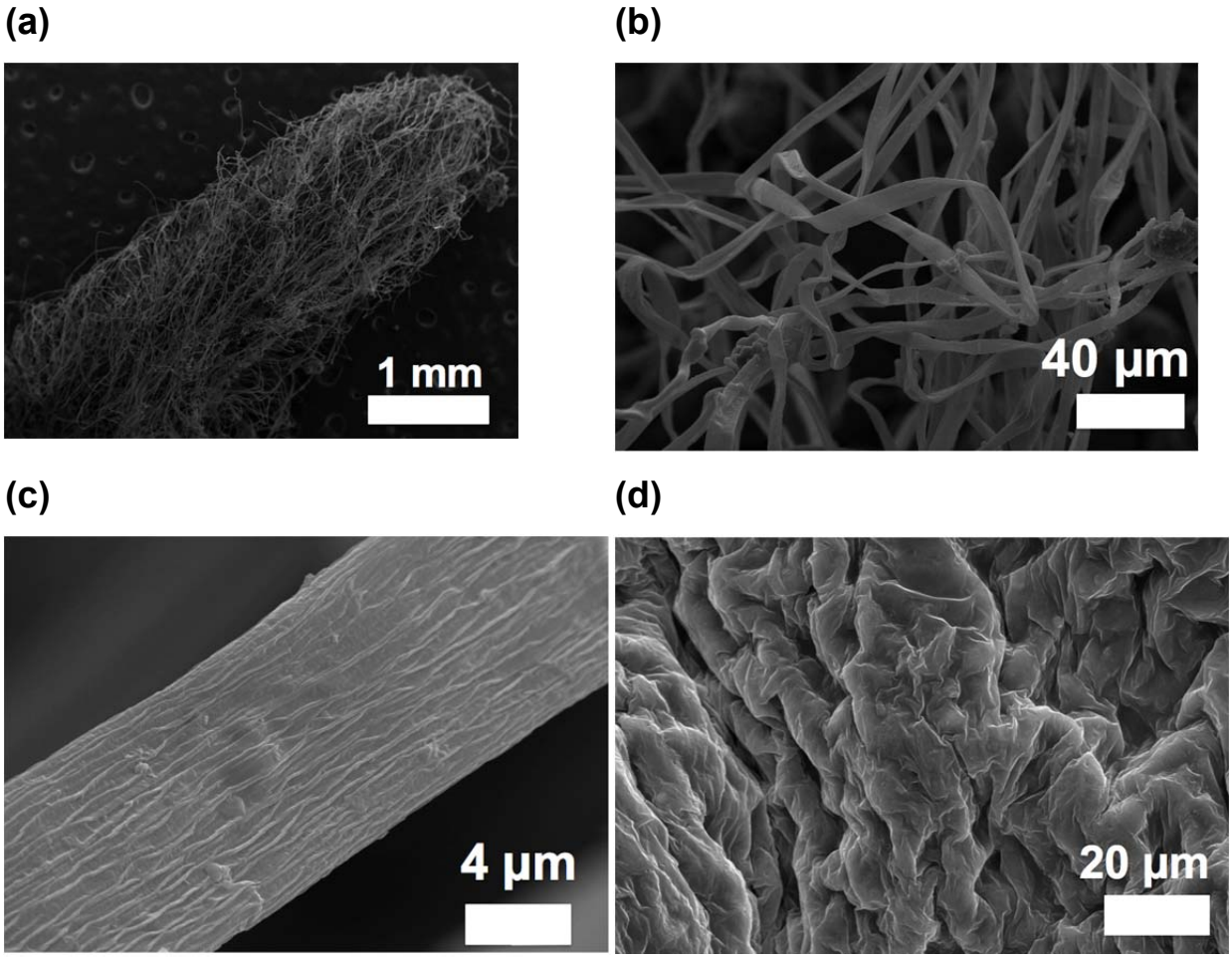

Figure 4: SEM images of *Salsola crassa*: (a) leaf with hairs; (b) fettuccine-like hairs; (c) individual hair; and (d) underlying leaf surface following hair removal.

3.2 Bioinspired Replication

Two generic types of readily available fibrous substrates were investigated: natural (cotton) and synthetic (non-woven polypropylene). The cotton fibres were 14.7 ± 4.0 µm in width, Figure 5. Whilst the non-woven materials comprised three variants: fine non-woven (5.0 ± 1.5 µm fibre diameter), coarse non-woven (22.4 ± 3.8 µm fibre diameter) held together by small melted regions (0.94 ± 0.10 mm separation), and a hierarchical-coarse (22.7 ± 4.4 µm fibre diameter) dimpled structure (0.68 ± 0.16 mm separation) chosen to mimic localised water channelling analogous to the *Salsola crassa* curled leaves directing collected water towards the plant's roots, Figure 2. All of these fibrous substrates were surface functionalised using either iCVD[19] or

plasmachemical[21,22] deposition without any visible alteration to their overall physical appearance, Supporting Information Figure S 1 and Figure S 2.

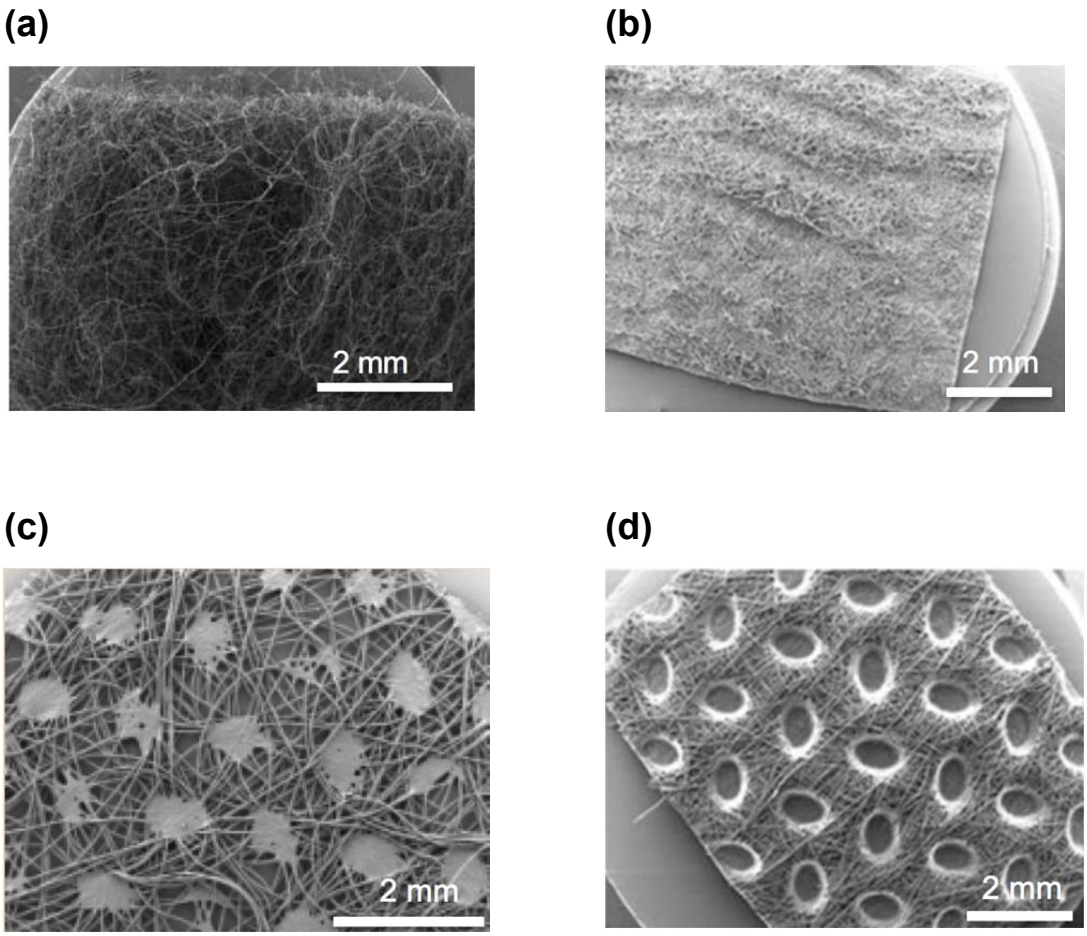

Figure 5: Low resolution SEM of: (a) cotton; (b) fine non-woven polypropylene; (c) coarse non-woven polypropylene; and (d) hierarchical-coarse non-woven polypropylene.

For the uncoated polyolefin fibre materials, a narrower fibre width (increase in surface area per unit mass) gives rise to an enhancement in water collection efficiency, which is simply due to the inherently higher surface areas of the finer size fibres, Figure 6 and Supporting Information Figure S 3.[30] In the case of the relatively similar fibre size coarse and hierarchical-coarse uncoated non-woven structures, the water contact angle (hence water collection efficiency) was lower for the latter, which is probably due to the length scale of the dimples interfering with the Cassie-Baxter enhancement of hydrophobicity[25].

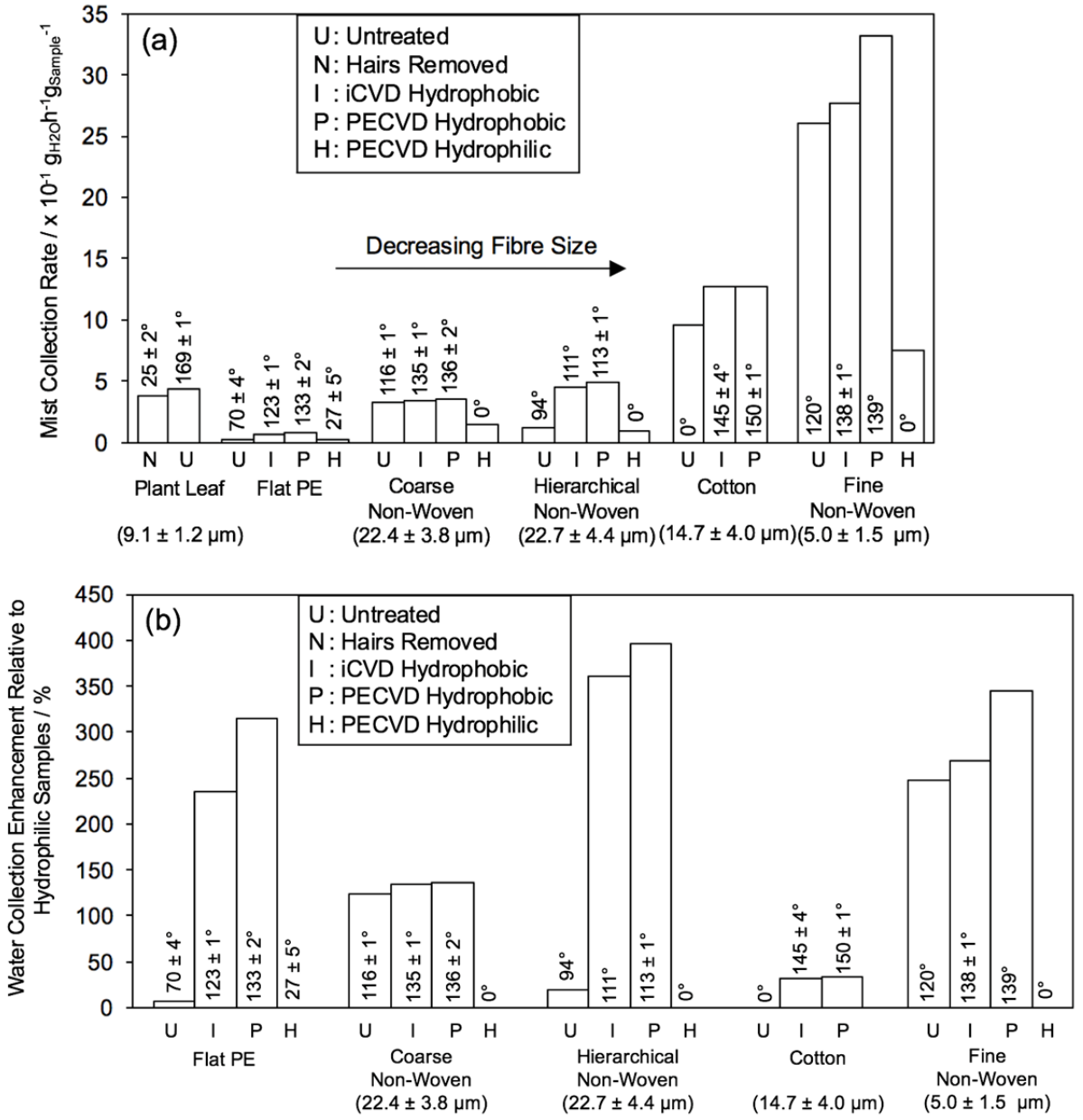

Figure 6: Mist collection of *Salsola crassa* plant with hairs, after hair removal, flat polyethylene sheet (reference), coarse non-woven polypropylene, hierarchical-coarse non-woven polypropylene, cotton, and fine non-woven polypropylene: (a) steady linear rate of water uptake beyond 60 min; and (b) steady linear rate of water collection (beyond 60 min) enhancement relative to complete wetting (hydrophilic functionalised) material (untreated in the case of cotton because it is already hydrophilic), Supporting Information Figure S 3 and Table S 1. Dimensions in brackets refer to fibre diameter.

Following the application of a hydrophilic coating onto the polyolefin fibres in order to enhance the surface wetting, lower water contact angles were measured compared to the reference polyolefin flat substrate, which can be attributed to the Wenzel effect[26], Figure 6. It was found that these lower water contact angles attenuated mist collection efficiencies.

Whereas in the case of hydrophobic functionalisation of the fibres (in order to mimic the leaf waxes of the plant *Salsola crassa*), there is an increase in water contact angle values due to the combination of a lower surface energy and the Cassie-Baxter effect[25], leading to a significant enhancement in water collection efficiencies (as high as over 300 percent), Figure 6. The narrowest fibres give rise to the most mist capture (even though the wider fibre coated cotton displays the highest water contact angle). This follows the trend observed for the uncoated polyolefin fibre materials, and highlights the importance of both fibre coating surface energy and effective surface area for mist collection.

A comparison of the rate of water collection relative to the corresponding hydrophilic surface for each type of material (i.e. normalisation for surface area) shows that an increase in hydrophobicity (water contact angle) leads to an enhancement in water collection efficiencies, Figure 6. Furthermore, the hierarchical dimpled surface shows the greatest enhancement in water collection compared to the single length scale (non-hierarchical) fibre materials. This suggests a synergistic effect of the hierarchical structure (collection and channelling of water), Figure 7. These meshes can be easily folded into various shapes including cones in order to mimic the overall three-dimensional fog collection behaviour observed for arid climate plant species such as *Salsola crassa* and *Cotula fallax*[16].

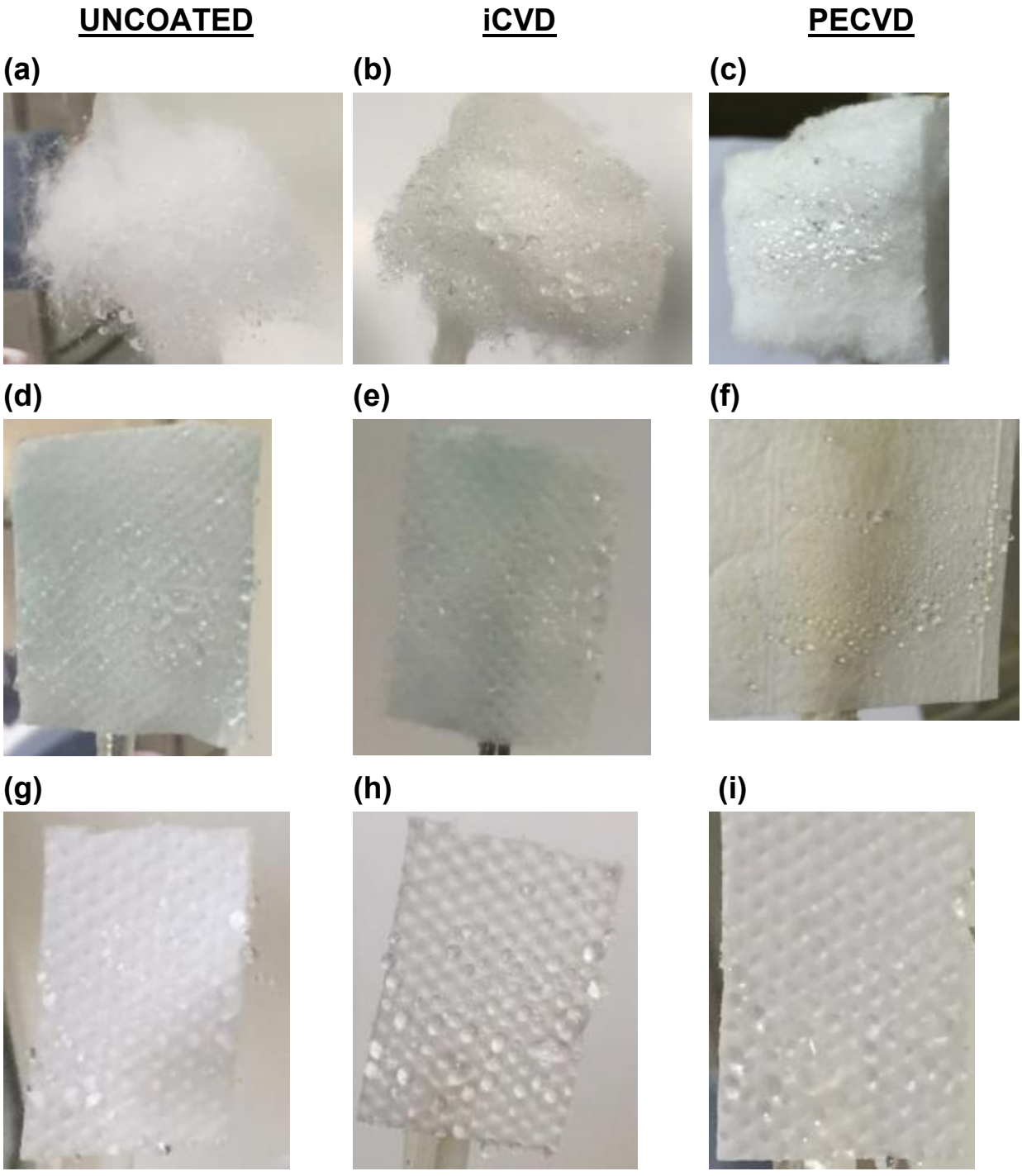

Figure 7: Photographs following exposure to mist for 2 h: (a–c) cotton; (d–f) fine non-woven polypropylene; and (g–i) hierarchical-coarse non-woven polypropylene. Note that for (g–i), water droplets are coalescing into the large scale regular patterned dimples (hierarchical). Width of samples is 30 mm.

4. DISCUSSION

Previous bioinspired porous structures for fog collection have included hydrophobic poly-l-lactic acid and hydrophilic polyvinyl alcohol membranes based upon spider silk (which stop performing after just 100 s of spray time due to the saturation of water collection)[27], bilayer hydrophilic-hydrophobic meshes inspired by *Berkheya purpurea* African thistles[28], and Janus hydrophobic copper mesh cylinder filled with hydrophilic cotton absorbent[29]; none of these offer any follow-on water channelling mechanism subsequent to fog collection. Whereas, the present hierarchical meshes exhibit a continual steady rate of fog collection beyond many hours without any detectable loss in efficiency, Supporting Information Figure S 3. The enhancement in efficiency observed by utilising a hydrophobic coating is consistent with previous studies employing conventional non-hierarchical 2-dimensional mesh structures[30,31], Figure 6.

The described hierarchical surface mist collection mechanism is also a good analogue to the previously reported mist collection behaviour of the *Cotula fallax* plant species, where plant hairs channel collected mist droplets into localised regions, leading to their growth and eventual fall due to gravity. The fog collection behaviours associated with the three-dimensional plant species, *Salsola crassa* and *Cotula fallax*[16] can be mimicked by folding the reported hierarchical fibrous material cloths into three-dimensional structures, or by their integration into architectural building designs (cones, funnels, roofing, e.g. by utilising a support grid[32]). It is envisaged that the adoption of such structures could overcome the disadvantages of conventional hanging two-dimensional fog harvesting nets, which are limited by their large size (due to low effective surface areas) and dependence upon wind directionality. Variants of the hierarchical fibrous cloths can be both natural and manmade materials (e.g. cotton and non-woven polypropylene respectively). For scale-up, roll-to-roll processing can be employed for the surface functionalisation of such materials. Beyond potable water, other potential uses could include the collection of water from power plant cooling towers[33] and agriculture[5,6,34].

5. CONCLUSIONS

An increase in hydrophobicity (lower surface energy) of fibrous meshes combined with a reduction in fibre diameter (higher surface area per unit mass) leads to enhanced mist collection efficiencies. For similar fibre sizes, a hierarchical structure gives rise to further improvement in mist collection which serves as a good mimic for arid climate *Salsola crassa* and *Cotula fallax* fog harvesting plant species.

6. ACKNOWLEDGEMENTS

This work was supported by Engineering and Physical Sciences Research Council (EPSRC) grant reference EP/J005401/1. S. N. Barrientos-Palomo was supported by Mexico CONACyT scholarship reference 409090. M. Gürsoy was supported by The Scientific and Technological Research Council of Turkey (TÜBITAK) - BIDEB National Doctoral Fellowship Program.

7. REFERENCES

1 The United Nations World Water Development Report 2012: Managing Water Under Uncertainty and Risk. Paris, UNESCO.

2 The United Nations World Water Development Report 2016: Water and Jobs. Paris, UNESCO.

3 Hamilton, W. J.; Seely, M. K. Fog Basking by the Namib Desert Beetle, *Onymacris unguicularis*. *Nature* **1976**, *262*, 284–285.

4 Klemm, O.; Schemenauer, R. S.; Lummerich, A.; Cereceda, P.; Marzol, V.; Corell, D.; van Heerden, J.; Reinhard, D.; Gherezghiher, T.; Olivier, J.; Osses, P.; Sarsour, J.; Frost, E.; Estrela, M. J.; Valiente, J. A.; Fessehaye, G. M. Fog as a Fresh-Water Resource: Overview and Perspectives. *Ambio* **2012**, *41*, 221–234.

5 Harb, O. M.; Salem, M. Sh.; Abd El-Hay, G. H.; Makled, Kh. M. Fog Water Harvesting Providing Stability for Small Bedwe Communities Lives in North Cost of Egypt. *Annals of Agricultural Sciences* **2016**, *61*, 105–110.

6 Potter, C. Measurements of Fog Water Interception by Shrubs on the California Central Coast. *J. Coastal Conserv.* **2016**, *20*, 315–325

7 Schemenauer, R. S.; Joe, P. I. The Collection Efficiency of a Massive Fog Collector. *Atmospheric Research* **1989**, *24*, 53–69

8 Regalado, C. M.; Ritter, A. The Design of an Optimal Fog Water Collector: A Theoretical Analysis. *Atmospheric Research* **2016**, *178–179*, 45–54.

9 Holmes R.; Rivera J. D. D.; de la Jara, E. Large Fog Collectors: New Strategies for Collection Efficiency and Structural Response to Wind Pressure. *Atmos. Res.* **2014**, *151*, 236–249.

10 Lee, J. J. Harvesting of Water from Fog Using Sponges. Master of Science thesis, University of Texas at Arlington, 2016.

11 Yang, H. R.; Zhu, H. J.; Hendrix, M. M. R. M.; Lousberg, N. J. H. G. M.; de With, G.; Esteves, A. C. C.; Xin, J. H. Temperature-Triggered Collection and Release of Water from Fogs by a Sponge-Like Cotton Fabric. *Adv. Mater.* **2013**, *25*, 1150–1154.

12 Bai, H.; Ju, J.; Sun, R.; Chen, Y.; Zheng, Y.; Jiang, L. Controlled Fabrication and Water Collection Ability of Bioinspired Artificial Spider Silks. *Adv. Mater.* **2011**, *23*, 3708−3711.

13 Azad, M. A. K.; Barthlott, W.; Koch, K. Hierarchical Surface Architecture of Plants as an Inspiration for Biomimetic Fog Collectors. *Langmuir* **2015**, *31*, 13172−13179.

14 Heng, X.; Xiang, M.; Lu, Z.; Luo, C. Branched ZnO Wire Structures for Water Collection Inspired by Cacti. *ACS Appl. Mater. Interfaces*, **2014**, *6*, 8032–8041.

15 Vogel, S.; Müller-Doblies, U. Desert Geophytes Under Dew and Fog: The “Curly-Whirlies” of Namaqualand (South Africa). *Flora* **2011**, *206*, 3–31.

16 Andrews, H. G.; Eccles, E. A.; Schofield, W. C. E.; Badyal, J. P. S. Three-Dimensional Hierarchical Structures for Fog Harvesting. *Langmuir* **2011**, *27*, 3798–3802.

17 Freitag, H.; Rilke, S. Salsola. In *Flora Iranica*; Rechinger, K. H., Ed.; Akademische Druck- und Verlagsanstalt; Graz, 1997, Vol. 172, pp. 154–255.

18 Toderich, K.N.; Shuyskaya, E.V.; Khujanazarov, T.M.; Ismail, S.; Kawabata, Y. The Structural and Functional Characteristics of Asiatic Desert Halophytes for Phytostabilization of Polluted Sites. In *Plant Adaptation and Phytoremediation*; Ashraf, M.; Oztur, K. M.; Ahmad, M. S. A. Eds.; Springer, 2010 pp 245-274.

19 Gürsoy, M.; Uçar, T.; Tosun, Z.; Karaman, M. Initiation of 2-Hydroxyethyl Methacrylate Polymerization by Tert-Butyl Peroxide in a Planar PECVD System. *Plasma Processes Polym.* **2016**, *13*, 438–446.

20 Gupta, M.; Gleason, K. K. Initiated Chemical Vapor Deposition of Poly(1H,1H,2H,2H-perfluorodecyl Acrylate) Thin Films. *Langmuir* **2006**, *22*, 10047–10052.

21 Coulson, S .R.; Woodward, I. S.; Brewer, S. A.; Willis, C.; Badyal, J. P. S. Ultra-Low Surface Energy Plasma Polymer Films. *Chem. Mater.* **2000**, *12*, 2031–2038.

22 Wood, T. J.; Schofield, W. C. E.; Lund, P.; Larsen, M. J.; Badyal, J. P. S. Highly Ion-Conducting Poly(Ionic Liquid) Layers. *Chem. Commun.* **2012**, *48*, 10201–10203.

23 Zak, J. A. Drop Size Distributions and Related Properties of Fog for Five Locations Measured From Aircraft. NASA Contractor Report 4585 DOT/FAA/CT-94/02, Langley Research Center, Virginia, USA. April 1994.

24 Azad, M. A.; Ellerbrok, D.; Barthlott, W.; Koch, K. Fog Collecting Biomimetic Surfaces: Influence of Microstructure and Wettability. *Bioinspir. Biomim.* **2015**, *10*, 016004.

25 Cassie, A. B. D.; Baxter, S. Wettability of Porous Surfaces. *Trans. Faraday Soc.* **1944**, *40*, 546–551.

26 Wenzel, R. N. Resistance of Solid Surfaces to Wetting by Water. *Ind. Eng. Chem.* **1936**, *28*, 988–994.

27 Du, M.; Zhao, Y.; Tian, Y.; Li, K.; Jiang, L. Electrospun Multiscale Structured Membrane for Efficient Water Collection and Directional Transport. *Small* **2016**, *12*, 1000–1005.

28 Shigezawa, N.; Ito, F.; Murakami, Y.; Yamanaka, S.; Morikawa, H. Development of Combination Textile of Thin and Thick Fiber for Fog Collection Bioinspired by Berkheya Purpurea. *J. Text. Inst.* **2016**, *107*, 1014–1021.

29 Cao, M.; Xiao, J.; Yu, C.; Li, K.; Jiang, L. Hydrophobic/Hydrophilic Cooperative Janus System for Enhancement of Fog Collection. *Small* **2015**, *11*, 4379–4384.

30 Park, K.-C.; Chhatre, S. S.; Srinivasan, S.; Cohen, R. E.; McKinley, G. H. Optimal Design of Permeable Fiber Network Structures for Fog Harvesting. *Langmuir*, **2013**, *29*, 13269–13277.

31 Rajaram, M.; Heng, X.; Oza, M.; Luo, C. Enhancement of Fog-Collection Efficiency of a Raschel Mesh using Surface Coatings and Local Geometric Changes. *Colloids and Surfaces A: Physicochemical and Engineering Aspects* **2016**, *508*, 218−229.

32 Trautwein, P. Fog Collector. *Patent* WO/2016/062877, April 28, 2016.

33 Ghosh, R.; Ray, T. K.; Ganguly, R. Cooling Tower Fog Harvesting in Power Plants – A Pilot Study. *Energy* **2015**, *89*, 1018−1028.

34 Hiatt, C.; Fernandez, D.; Potter, C. Measurements of Fog Water Deposition on the California Central Coast. *Atmospheric and Climate Sciences* **2012**, *2*, 525–531.

Bioinspired Fog Capture and Channel Mechanism Based on the Arid Climate Plant *Salsola crassa*

(Supplementary Material)

M. Gürsoy[a], M. T. Harris[b], J. O. Downing[b], S. N. Barrientos-Palomo[b], A. Carletto[b], A. E. Yaprak[c], M. Karaman[a†], and J. P. S. Badyal[b†*]

[a] Chemical Engineering Department, Selçuk University, Konya 42075, Turkey

[b] Chemistry Department, Science Laboratories, Durham University, Durham DH1 3LE, England, UK

[c] Department of Biology, Faculty of Science Ankara University, Ankara 06100, Turkey

† These authors have made equal contributions.

* Corresponding author email: j.p.badyal@durham.ac.uk

1. FIGURES

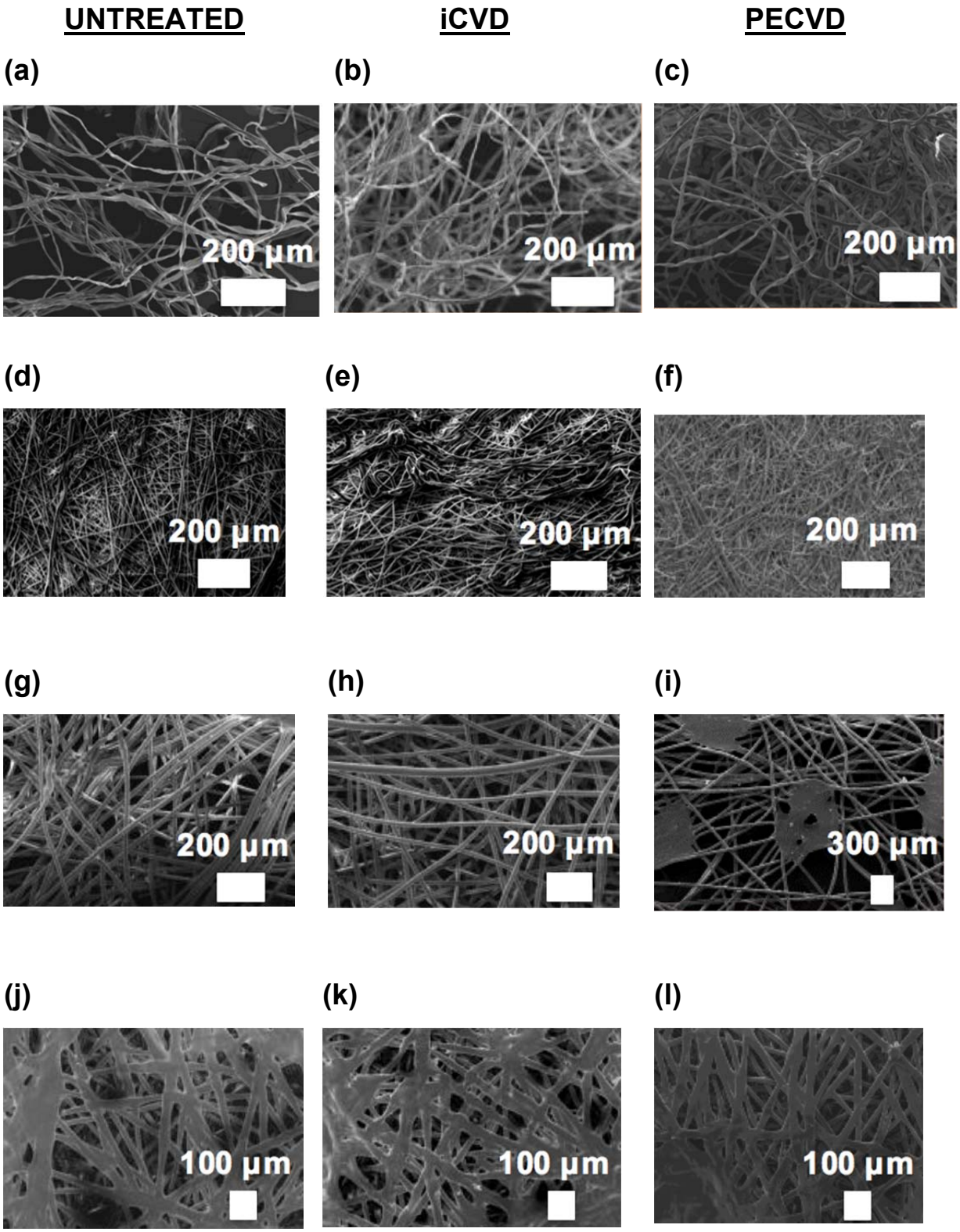

Figure S 1: Medium resolution SEM of: (a–c) cotton; (d–f) fine non-woven polypropylene; (g–i) coarse non-woven polypropylene; and (j–l) hierarchical-coarse non-woven polypropylene dimpled region.

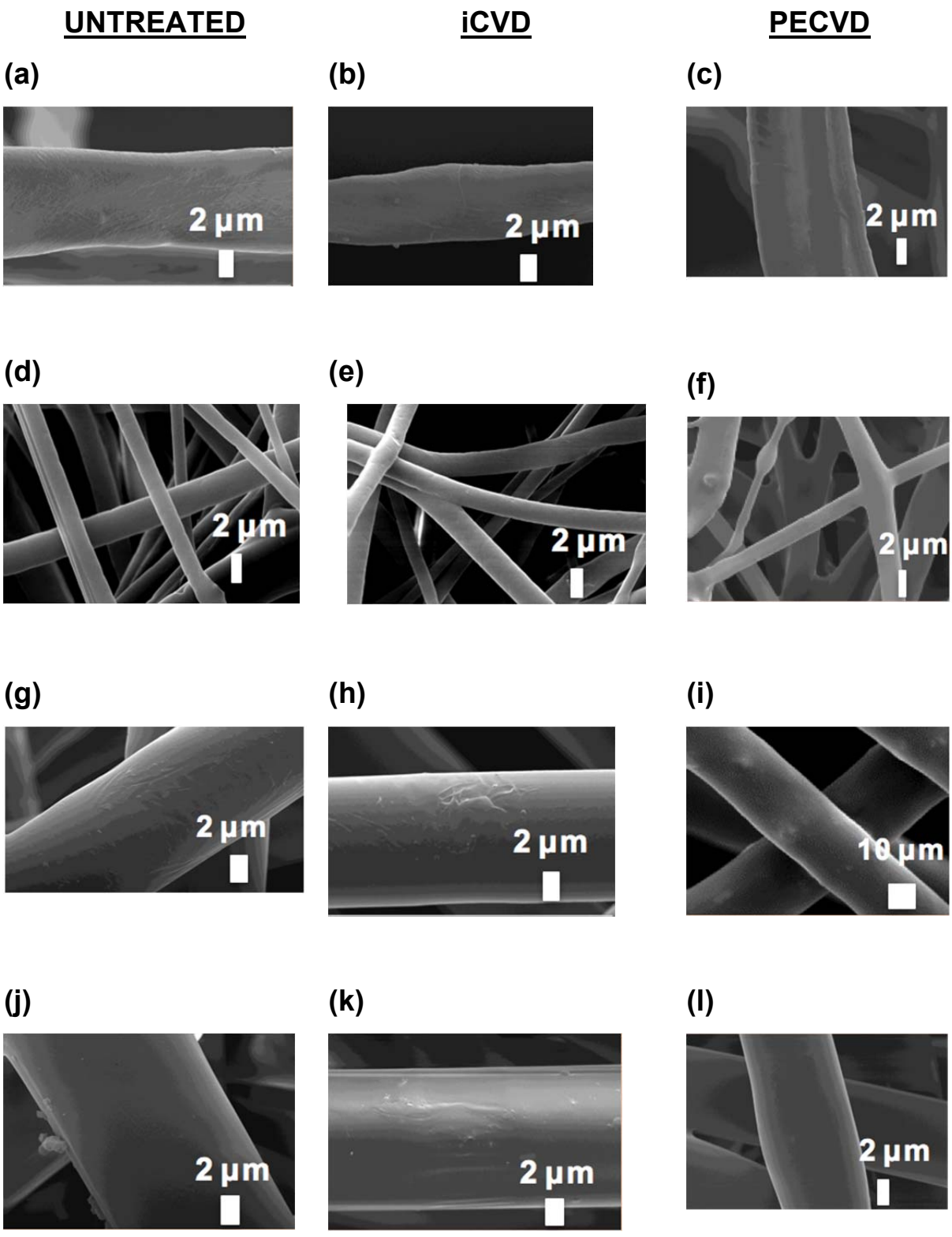

Figure S 2: High resolution SEM of: (a–c) cotton; (d–f) fine non-woven polypropylene; (g–i) coarse non-woven polypropylene; and (j–l) hierarchical-coarse non-woven polypropylene dimpled region.

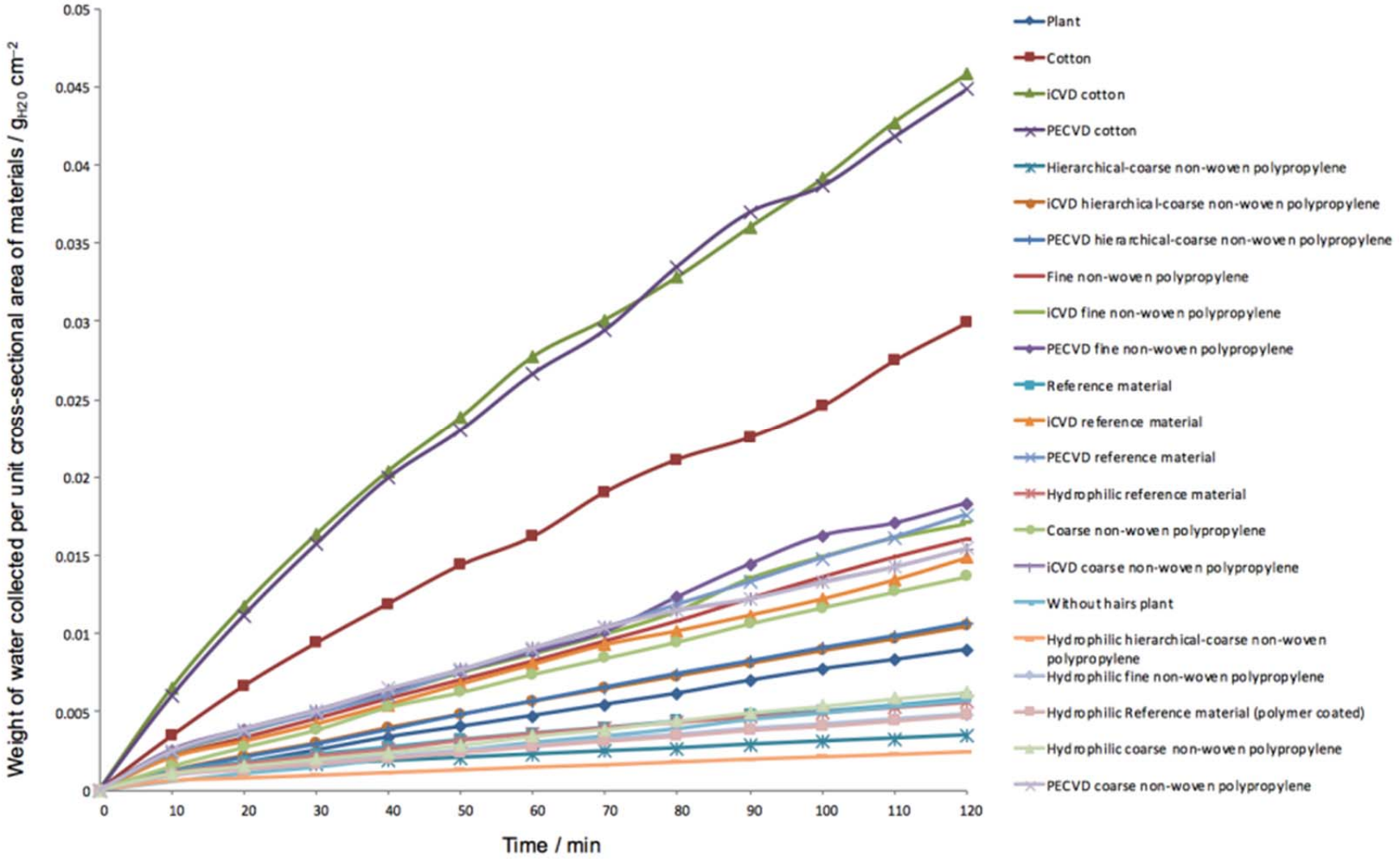

Figure S 3: Water collection onto different materials normalised to per unit area facing mist.

2. TABLE

Table S 1: Contact angle and linear rate of water uptake beyond 60 min.

Material (Average Fibre Diameter)	Treatment	Frontal area / cm^2	Sample Mass / g	Contact Angle / °	Water Collection / x 10^{-2} g_{H2O} h^{-1} g_{Sample}^{-1}	Water Collection Enhancement Relative to Untreated / %	Water Collection Enhancement Relative to Hydrophilic Sample
Salsola crassa plant with hairs	Untreated	3.8	0.0365	169 ± 1	43.8 ± 0.8		
Same *Salsola crassa* plant sample without hairs	Untreated	1.98	0.01392	25 ± 2	38.1 ± 0.7		
Reference material	Untreated	9	0.984	70 ± 4	2.1 ± 0.0	0%	7%
	iCVD - Hydrophobic	9	0.975	123 ± 1	6.3 ± 0.3	210%	235%
	PECVD - Hydrophobic	9	0.992	133 ± 2	7.8 ± 0.2	291%	314%
	PECVD - Hydrophilic	9	0.949	27 ± 5	1.9 ± 0.1	-6%	0%
Coarse non-woven polypropylene (22.40 ± 3.84 µm)	Untreated	9	0.171	116 ± 1	33.0 ± 0.5	0%	123%
	iCVD - Hydrophobic	9	0.165	135 ± 1	34.6 ± 0.9	5%	134%
	PECVD - Hydrophobic	9	0.164	136 ± 2	34.9 ± 0.7	6%	136%
	PECVD - Hydrophilic	9	0.172	0	14.8 ± 0.4	-55%	0%
Hierarchical-coarse non-woven polypropylene (22.69 ± 4.38 µm)	Untreated	9	0.092	94 ± 1	11.9 ± 1.2	0%	20%
	iCVD - Hydrophobic	9	0.092	111 ± 1	45.2 ± 3.8	273%	360%
	PECVD - Hydrophobic	9	0.0918	113 ± 1	48.9 ± 2.4	312%	397%
	PECVD - Hydrophilic	9	0.0894	0	9.9 ± 0.2	-17%	0%
Cotton (14.73 ± 4.04 µm)	Untreated	9	0.1287	0†	95.7 ± 5.1	0%	0%
	iCVD - Hydrophobic	9	0.128	145 ± 4	127.0 ± 3.3	32%	32%
	PECVD - Hydrophobic	9	0.1278	150 ± 1	127.9 ± 6.5	33%	33%
Fine non-woven polypropylene (5.04 ± 1.51 µm)	Untreated	9	0.0269	120 ± 1	260.60 ± 6.0	0%	248%
	iCVD - Hydrophobic	9	0.0272	138 ± 1	276.1 ± 22.6	7%	269%
	PECVD - Hydrophobic	9	0.0258	139 ± 1	332.2 ± 6.8	22%	344%
	PECVD - Hydrophilic	9	0.0242	0	74.8 ± 6.0	-71%	0%

†Absorbs water